Poly(lactide-co-glycolide)-rifampicin nanoparticles efficiently clear *Mycobacterium bovis* BCG infection in macrophages and remain membrane-bound in phago-lysosomes

Raja Kalluru[1,*], Federico Fenaroli[1,*], David Westmoreland[1,*], Lilia Ulanova[1], Atoosa Maleki[2], Norbert Roos[1], Marie Paulsen Madsen[1], Gerbrand Koster[1], Wolfgang Egge-Jacobsen[1], Steven Wilson[2], Hanna Roberg-Larsen[2], Gopal K. Khuller[3], Amandeep Singh[3], Bo Nyström[2] and Gareth Griffiths[1,‡]

[1]Department of Molecular Biosciences, University of Oslo, 0316 Oslo, Norway
[2]Department of Chemistry, University of Oslo, 0315 Oslo, Norway
[3]Department of Biochemistry, Postgraduate Institute of Medical Education and Research, 160012 Chandigarh, India

*These authors contributed equally to this work
‡Author for correspondence (garetg@imbv.uio.no)

Accepted 16 April 2013
Journal of Cell Science 126, 3043–3054

doi: 10.1242/jcs.121814

Summary

Nanoparticles (NPs) are increasingly used as biodegradable vehicles to selectively deliver therapeutic agents such as drugs or antigens to cells. The most widely used vehicle for this purpose is based on copolymers of lactic acid and glycolic acid (PLGA) and has been extensively used in experiments aimed at delivering antibiotics against *Mycobacterium tuberculosis* in animal models of tuberculosis. Here, we describe fabrication of PLGA NPs containing either a high concentration of rifampicin or detectable levels of the green fluorescent dye, coumarin-6. Our goal here was twofold: first to resolve the controversial issue of whether, after phagocytic uptake, PLGA NPs remain membrane-bound or whether they escape into the cytoplasm, as has been widely claimed. Second, we sought to make NPs that enclosed sufficient rifampicin to efficiently clear macrophages of infection with *Mycobacterium bovis* BCG. Using fluorescence microscopy and immuno-electron microscopy, in combination with markers for lysosomes, we show that BCG bacteria, as expected, localized to early phagosomes, but that at least 90% of PLGA particles were targeted to, and remained in, low pH, hydrolase-rich phago-lysosomes. Our data collectively argue that PLGA NPs remain membrane-enclosed in macrophages for at least 13 days and degrade slowly. Importantly, provided that the NPs are fabricated with sufficient antibiotic, one dose given after infection is sufficient to efficiently clear the BCG infection after 9–12 days of treatment, as shown by estimates of the number of bacterial colonies *in vitro*.

Key words: Nanoparticles, Mycobacteria, Macrophages

Introduction

Tuberculosis (TB) caused by *Mycobacterium tuberculosis* (M.tb) has again developed into a major health problem, with 1.7 million deaths every year and a staggering 2 billion latently infected (Young et al., 2008). Despite enormous efforts, a successful vaccine is not available and a consensus has emerged that the century-old BCG vaccine is ineffective (Dye and Williams, 2010). Provided the bacteria are not multidrug resistant, the disease can be effectively treated with the so-called 'short course' regime, actually 6–8 months of treatment with a combination of four antibiotics: rifampicin, isoniazid, pyrazinamide and ethambutol. When the bacteria are multi-drug resistant the efficiency of antibiotic therapy decreases significantly, thus more toxic 'second-line' antibiotics have to be used, generally for up to 24 months, using up to six different drugs. Patient non-compliance is a significant problem (Zhang and Yew, 2009).

Some general problems with the application of most medicinal drugs are that: (1) The drugs not only reach the target cells and tissues of interest, but also become distributed systemically throughout the body. (2) Most drugs are rapidly degraded or excreted, usually within hours. (3) Some drugs have limited bioavailability and are poorly absorbed via, for example, the oral route (Sosnik et al., 2010).

Over the past two decades an exciting alternative concept for drug delivery has been developed using nanotechnology (Couvreur and Vauthier, 2006; Danhier et al., 2012), and especially to encapsulate the drugs inside slowly biodegradable, polymer nanoparticles (NPs). The goal then is to selectively target the diseased cells. For example, in approaches against cancer one would attach a molecule, such as an antibody to the NPs that selectively binds to specific target molecules on the surface of the cancer cells (Davis et al., 2008).

A particularly attractive feature of considering a NPs approach against M.tb is that these bacteria are predominantly intracellular residents of macrophages. These are also the cells that function most efficiently in taking up many kinds of particles from the blood circulation via phagocytosis – provided they are above about 0.2 μm in diameter (Desjardins and Griffiths, 2003). It follows that when NPs or micro-particles (MPs) (>1000 nm) enclosing antibiotics are able to access the circulatory system of

Journal of Cell Science

mammals infected with M.tb the particles can be efficiently taken up into the M.tb-infected macrophages. There, the polymer is degraded, allowing the drugs to be released locally and directly into the infected cell in a sustained fashion. A number of groups have published impressive data using different types of polymer NPs and MPs enclosing different antibiotics against mycobacteria in a range of different mammalian tuberculosis model systems (see review by Pandey and Khuller, 2006). Most of these studies have used the polymer poly(lactic-co-glycolic acid) (PLGA), while a few have used chitosan or alginate (Pandey and Khuller, 2004; Ul-Ain et al., 2003).

Among the most striking results in the field of TB are data directly comparing conventionally administered anti-M.tb antibiotics (via the oral or lung-inhalation routes) with the PLGA-enclosed antibiotics. In guinea pigs, for example, 46 daily doses of free antibiotics were required to clear the animals of infection. In contrast, only 3–5 doses of NP-enclosed antibiotics were needed for complete therapy. The blood levels of rifampicin, isoniazid and pyrazinamide in infected guinea pigs remained significant for only a few hours after conventional drug treatment. In contrast, with NP-based treatment the antibiotics remained in the circulation at concentrations above the minimum-inhibitory concentration needed to kill M.tb for over a week (Pandey et al., 2003; Sharma et al., 2004b).

Although there are convincing therapeutic data against M.tb in macrophages with both sub-500 nm NPs containing anti-mycobacterial drugs (Muttil et al., 2007; Sharma et al., 2004a) and >1000 nm MPs (Muttil et al., 2007; Yoshida et al., 2006) it is generally accepted that *in vivo* the smaller NPs are more efficient at crossing epithelial barriers non-invasively, for example after lung inhalation or oral administration (Hussain et al., 2001). We therefore put great effort in producing uniform-sized NPs where the bulk of particles were below 400 nm.

Here, we focused on the mechanisms by which PLGA rifampicin NPs interacted with primary macrophages infected with *M. bovis* BCG. This well-characterized mycobacterium has been extensively used for anti-TB vaccination. BCG behave like M.tb in that, after entry into macrophages they remain inside phagosomes whose maturation is blocked at an early stage – before the hydrolytic phago-lysosome stage (Rohde et al., 2007). However, in contrast to M.tb, which multiplies in these cells, BCG neither grows, nor is significantly killed by the macrophages (Jordao et al., 2008).

A number of studies have addressed the interactions of rifampicin PLGA MPs or NPs with primary macrophages, or macrophage cell lines infected with mycobacteria, including M.tb (Anisimova et al., 2000; Barrow et al., 1998; Hirota et al., 2010; Makino et al., 2004; Quenelle et al., 2001; Sharma et al., 2001; Yoshida et al., 2006). Other antibiotics, such as moxifloxacin, combined with other polymers (polybutyl-cyanoacrylate, PBCA), have also been successfully used for NP-based therapy of M.tb in macrophages (Kisich et al., 2007). Crucially, after MPs are given to macrophages the intracellular concentration of the antibiotic in macrophages can be up to 25-fold enriched compared to that outside these cells. Similarly, when compared to the administration of free rifampicin, the particle approach also can give up to a 20-fold higher concentration in the macrophages (Anisimova et al., 2000; Hirota et al., 2010; Makino et al., 2004; Sharma et al., 2007; Sharma et al., 2001). Overall, the NPs/MPs approach leads to a more effective therapy at the *in vitro* cell level, in agreement with the mammalian animal model studies cited above.

A few of these cell-level studies have also encapsulated a fluorescent dye (without antibiotics) inside PLGA or other polymer particles, in order to follow their localization in cells (Jain et al., 2010; Kisich et al., 2007; Onoshita et al., 2010). The Kisich et al. study (Kisich et al., 2007) infected macrophages with Oregon Green surface-labeled M.tb and additionally internalized rhodamine-labeled polybutyl-cyanoacrylate PBCA particles. It was reported that there was no visible colocalization of NPs and bacteria. In the paper by (Onoshita et al., 2010), between 80 and 90% of the PLGA MPs enclosing the green fluorescent dye coumarin-6, colocalized with vesicles labeled with the low pH vital dye LysoTracker Red for at least 7 days in a rat alveolar macrophage cell line. It is agreed in the field that only a small fraction of M.tb (and BCG) are found in LysoTracker-positive late endosomes and lysosomes (simplified in the rest of this paper collectively as 'lysosomes') in macrophages (Jordao et al., 2008). These data collectively suggest that while the M.tb can stay in an arrested early phagosome that has a pH of around 6.2 (Rohde et al., 2007), the subsequently phagocytosed MPs can traffic to the phago-lysosome compartment, where the polymer is slowly degraded.

The above scenario is, however, at odds with the widely cited papers of Panyam et al. (Panyam et al., 2003; Panyam et al., 2002) and (Panyam and Labhasetwar, 2003a; Panyam and Labhasetwar, 2003b) who claimed that PLGA NPs are able to exit rapidly – within minutes – from endocytic/phagocytic compartments of a human smooth muscle cell line (see for example Danhier et al., 2012 that accepts this scenario as an established fact). Other publications have come to the same conclusion that the intact PLGA NPs/MPs 'escape' from the endocytic pathway to the cytoplasm in different cell types, including macrophages (Gomes et al., 2006), HeLa cells (Cheng et al., 2008), dendritic cells and B-cells (Shen et al., 2006), and epithelial cells (Cartiera et al., 2009). These studies relied on light microscopy immunofluorescence analyses and another EM study reached the same conclusion (Mathiowitz et al., 1997). In contrast, (Schliehe et al., 2011) concluded that in dendritic cells, PLGA MPs remained in phago-lysosomes for many days. Given these contradictory results we wanted to establish more definitively here whether or not PLGA NPs of different sizes remain long-term in membrane-enclosed phagocytic/endocytic compartments, or whether they are able to disrupt the enclosing membrane and escape into the cytoplasm.

Here, we developed a method to encapsulate either rifampicin or coumarin-6 in PLGA NPs. We subsequently carried out a detailed light microscopy and immuno-EM analysis of the localization of the green NPs and red BCG in both mouse bone macrophages and the RAW mouse macrophage cell line. Our results show unequivocally that the BCG bacteria indeed do not colocalize with the subsequently administered PLGA NPs. The vast majority of the NPs were in phago-lysosomes. Finally, provided we encapsulated sufficient rifampicin, the NPs were able to effectively clear the macrophages of the BCG, as shown by estimation of colony forming units.

Results

Fabrication and characterization of PLGA nanoparticles

Two different methods of preparation were used to produce NPs of different size ranges, as monitored by negative staining TEM,

fluorescence microscopy, and scanning EM (Fig. 1); the surface of the particles were relatively smooth, as seen by SEM (Fig. 1E,F) and by cryo-TEM (supplementary material Fig. S1). When the NPs were prepared by the standard method (method A; see Materials and Methods) they exhibited a size distribution ranging from 50 nm up to 2 µm, as seen in Fig. 1A,C,E. However, when NPs were prepared using selective centrifugation (method B; Fig. 1B,D,F) they exhibited a much narrower size distribution range, predominantly between 50 nm and 400 nm. However, a price to pay for this improved size distribution was a significantly lower yield of NPs, relative to the standard method. We, therefore, only used these NPs for a few selected experiments (indicated below).

NPs required for slow drug release were prepared by carefully controlling the evaporation rate of dichloromethane (DCM), a highly volatile solvent (see Materials and Methods). Using this controlled evaporation method we managed to obtain NPs with more than 30% drug encapsulation.

We initially put great effort in co-encapsulating both detectable levels of coumarin-6 and high concentration of rifampicin in the same PLGA NPs. However, when the coumarin-6 dye was also included in the NPs, this significantly reduced the amount of encapsulated rifampicin, probably due to a competition between the two molecules during the evaporation of the solvent. We managed, at best to achieve around 10% loading of rifampicin, that was too low for the therapy experiments (see

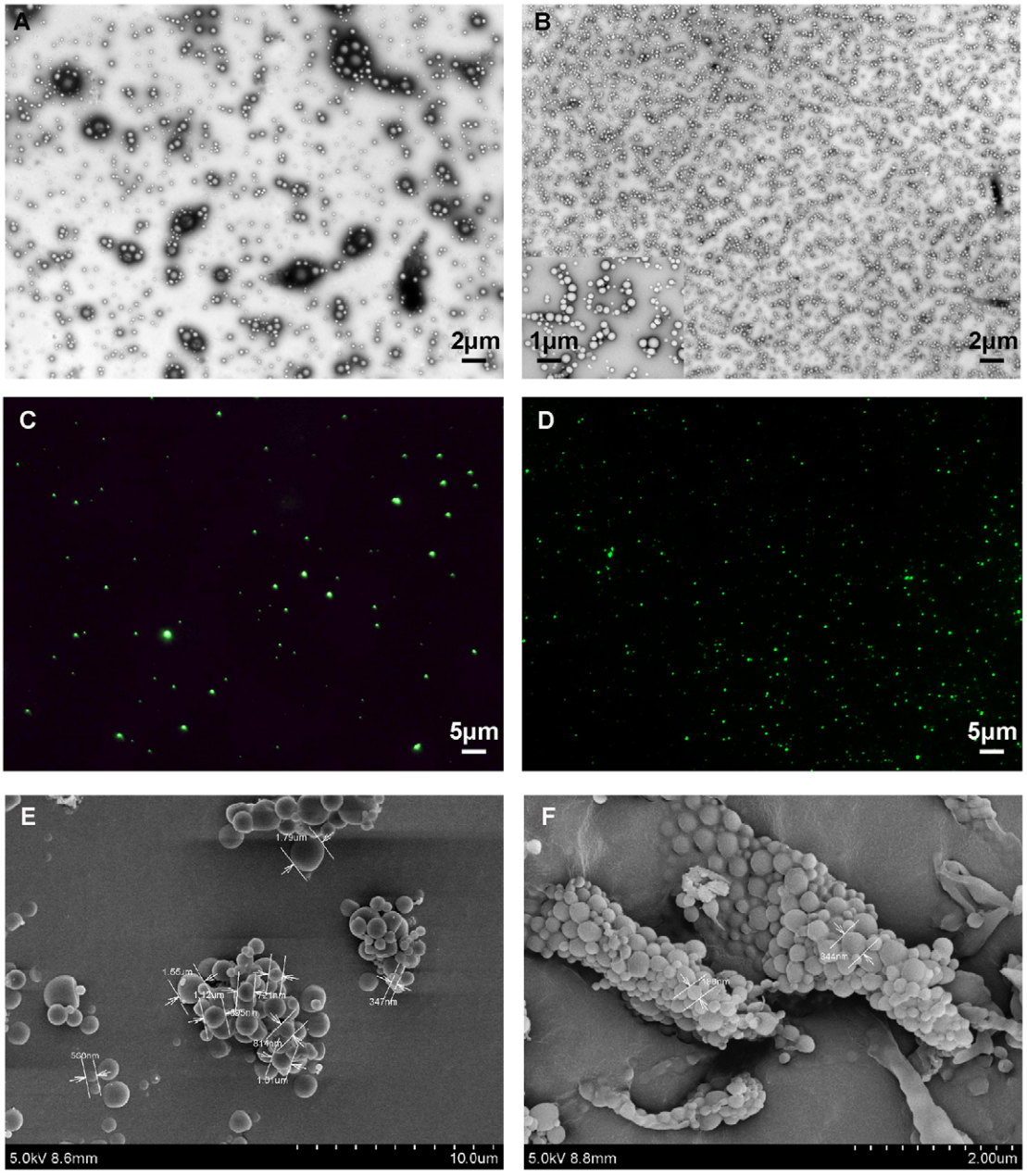

Fig. 1. Microscopy of nanoparticles. (**A–F**) Images obtained using TEM (A,B), confocal microscopy (C,D) and SEM (E,F). A, C and E show NPs made with the standard preparation method. B, D and F show the NPs prepared after selective centrifugation.

Table 1. Physical and chemical characteristics of selected batches of NPs

Batch	Preparation	NP loading*	Size† (nm)	β-value†	Z-potential (mV)
1	Standard method	N.D.	118±2	0.97	−4.28±0.3
2	Selective centrifugation	Coumarin-6 (1%)	316±3	0.96	N.D.
3	Standard method	Rifampicin (31%)	228±5	0.94	−3.14±0.2
4	Standard method	Rifampicin (1%)	N.D.	N.D.	N.D.

The autocorrelation functions, $g^1(t)$, were fitted with the aid of a stretched exponential, $g^{(1)}=\exp[-(t/\tau_{fe})^{\beta}]$, where τ_{fe} is an effective relaxation time and β ($0<\beta\leq1$) is a measure of the width of the distribution of relaxation times. The high vales of β suggest narrow size distributions of the particles. All size measurements were done after lyophilization. N.D., not determined.

*Loading is given as % by weight (w/w).

†As determined from DLS measurements.

below) (Results not shown). We therefore used separate types of NPs for the coumarin-6 and the rifampicin for the rest of this study.

Table 1 summarizes the data on a selection of NPs with respect to rifampicin and coumarin-6 loading, size and β-values (giving information about the particle size distribution) determined from dynamic light scattering and zeta potential. More details about the analyses of the DLS data have been given previously (Kjøniksen et al., 1999). These results confirm that the NPs are slightly negatively charged (under conditions of 0.15 M NaCl) and are uniform in size distribution.

In one experiment we estimated the *in vitro* release of rifampicin from NPs loaded (at 33.5%) with rifampicin that was incubated either with HEPES buffer pH 7.4 or acetate buffer pH 4 (to simulate conditions in lysosomes). We observed a rapid release in the first day (at pH 7.4) and a slower release subsequently until the experiment was terminated after 12 days (supplementary material Fig. S2). A slightly slower release was seen at pH 4. However, as pointed out by Makino et al. rifampicin is less soluble at pH 4 than at pH 7 (Makino, 2004). Our results are essentially identical to figure 2 in the study of Onoshita and co-workers using PLGA-rifampicin NPs (Onoshita, 2010).

BCG and NP co-incubation in macrophages

We initially investigated the uptake of the PLGA NPs containing coumarin-6 into the RAW mouse macrophage cell line, both with and without infection with DS-Red BCG. Due to the rapid cell division of the RAW macrophage cell line, only a small fraction of cells were found to contain NPs or BCG bacteria after 7–9 days. Although we still used RAW cells for specific experiments (up to 3 days), for most of the subsequent studies we used mouse bone marrow-derived primary macrophages (BMDM). At 6–7 days after isolation these cells do not divide significantly; this allowed us to carry out infection/NP studies for a further 12–15 days.

The uptake of PLGA-NPs was followed in primary macrophages that were first infected with BCG. For this, the macrophages were incubated for 3 hours with DS-Red BCG, at a concentration that gave us, on average 1–10 bacteria/cell, as determined by fluorescence microscopy (Fig. 2). After a chase period without bacteria, three different concentrations (25, 50 and 100 μg/ml) of the PLGA NPs containing coumarin-6 were added for a further 3 hours before washing with PBS. These cells were kept in culture for a further 12–15 days.

As shown in Fig. 2A,B, at all times after infection we found that bacteria and NPs are taken up by the same cells, but essentially none of the red bacteria colocalized with the green NPs under all conditions, irrespective of bead size. The same result was obtained with GFP-BCG, in combination with rhodamine-labeled PLGA NPs (results not shown).

NPs are targeted to a low pH, protease-rich phago-lysosome compartment

After infection with BCG or M.tb, the vast majority of the bacteria reside in an arrested early phagosome stage (e.g (Jordao et al., 2008)). We confirmed this using LysoTracker Red dye that accumulates in intracellular compartments with a pH lower than around 5.5; the vast majority of BCG bacteria were found in LysoTracker-negative compartments (Fig. 2C–E).

We asked whether the NPs enclosing coumarin-6, that were added to cells after infection with BCG, could bypass the arrested BCG early phagosome compartment and be delivered to a late endocytic compartment. Since most of the NPs prepared according to the standard method are larger than the expected minimum size (200 nm) considered necessary for the process of phagocytosis (Desjardins and Griffiths, 2003) we assume that the NPs are mainly entering the macrophage by phagocytosis; however, this issue was not addressed further.

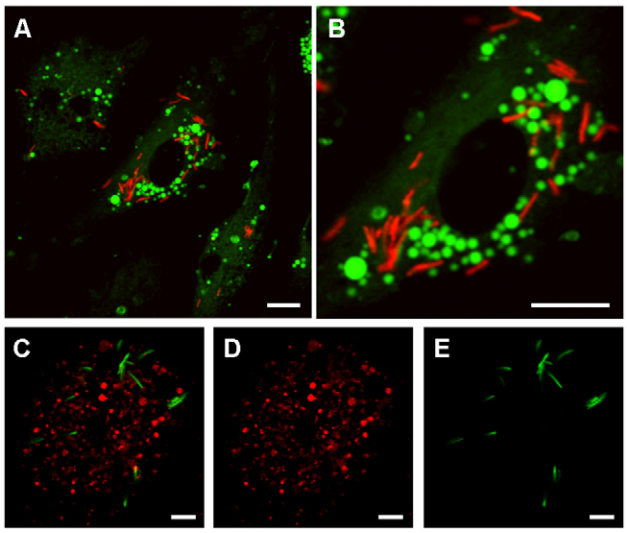

Fig. 2. PLGA particles and BCG do not colocalize and BCG is not in Lysotracker-Red-positive compartments. (**A**) Localization by fluorescence micrscopy of PLGA NPs (green) and DS-Red BCG in primary macrophages after 1-day internalization. (**B**) Higher magnification of a cell in A. (**C–E**) GFP (green) BCG after 1-day internalization in cells labeled for LysoTracker Red: overlap image (C); LysoTracker channel (D); GFP bacteria channel (E). Scale bars: 10 μm (A,B); 5 μm (C,D).

As shown in Fig. 3A and Table 2, all the intracellular NPs, irrespective of size, consistently colocalized with LysoTracker, after 1 day, and up to 7 days incubation, indicating that they reside a long time in acidic phago-lysosomes.

Further evidence supporting the localization of the NP to phago-lysosomes came with the use of DQ-Red-BSA (DQ) that was allowed to enter cells by endocytosis. DQ-Red is a red bodipy dye linked to a BSA as a protease substrate such that, in the absence of hydrolysis, the fluorochrome self-quenches. However, when the compound is exposed to proteases the quenching is relieved, leading to a red fluorescence signal in protease-positive organelles, presumed to be the lysosomes (Molecular Probes data sheet). As shown in Fig. 3B the vast majority of coumarin-6 NPs internalized into primary macrophages colocalized with the red signal indicative of protease activity; a quantitative estimate in these cells showed that around 90% of the NPs colocalized with the dye (Table 2). Similar results were seen in RAW macrophages (data not shown).

We also asked whether the compartment in which the green NPs accumulates at steady state, is positive for the late endosome/lysosome membrane marker LAMP 2, using immunofluorescence microscopy. The majority of the NPs labeled structures appeared to have LAMP 2 labeling on their periphery; this was most evident with larger NPs (Fig. 3C). This labeling was quantified more precisely by immuno-EM (below).

Breakdown of PLGA NPs

PLGA particles are known to be degraded slowly over many days or even weeks in water via hydrolysis of their ester linkages (Makadia and Siegel, 2011). We conducted a set of experiments to follow the rate of loss of the coumarin-6 fluorescent signal from the PLGA-coumarin-6 NPs (without rifampicin) in primary macrophages. The NPs were internalized into the cells for 3 hours and then washed and chased for up to 13 days. The cells were imaged by confocal microscopy using identical imaging settings for all time points. The first image (day 0) was taken 3 hours after addition of the particles and subsequently we took images at selected time-points up to 13 days. As shown in Fig. 4, the average grey value [total fluorescence divided by the number of cells (number of nuclei)] decreased gradually over the time period, with only hints of a signal in NPs remaining at the final time point panel. A quantification of the imaging data are shown in Fig. 4, lower right panel. The fluorescence intensity decreases exponentially with time until it is close to background noise at day 13 [decay lifetime from fit: 4.2 days (fit-error 0.13 days)]. In separate measurements of the same set of images, we measured the mean fluorescence of the cytoplasm (i.e. areas in the cell *not* containing NPs). This signal was also lost exponentially with lifetime 6.3 days (fit-error 1.8 days) (supplementary material Fig. S3). The simplest interpretation of these results is that the NPs in phago-lysosomes are gradually hydrolyzed, releasing the

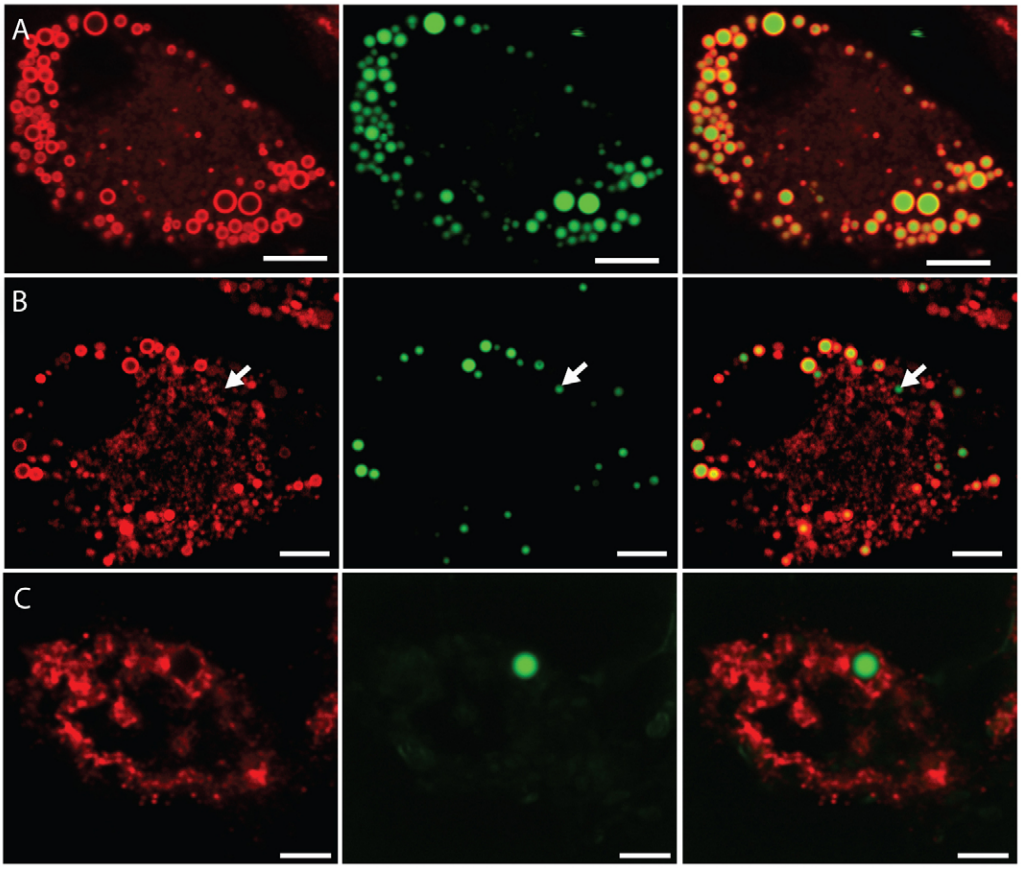

Fig. 3. PLGA particles are in phago-lysosmal compartments in primary macrophages. (**A**) Colocalization of NP (green) and LysoTracker Red in the same vesicles in live-cell primary macrophages after 1 day of NP internalization. (**B**) Colocalization of NPs (green) with DQ-Red BSA staining in live-cell primary macrophages after 1 day of NP internalization. The arrowhead indicates one NP that does not colocalize with the DQ. (**C**) Immunofluorescence labeling for LAMP-2 (red) in fixed cells after 1 day of green NP internalization; the label is concentrated around a large PLGA particle. Scale bars: 5 μm.

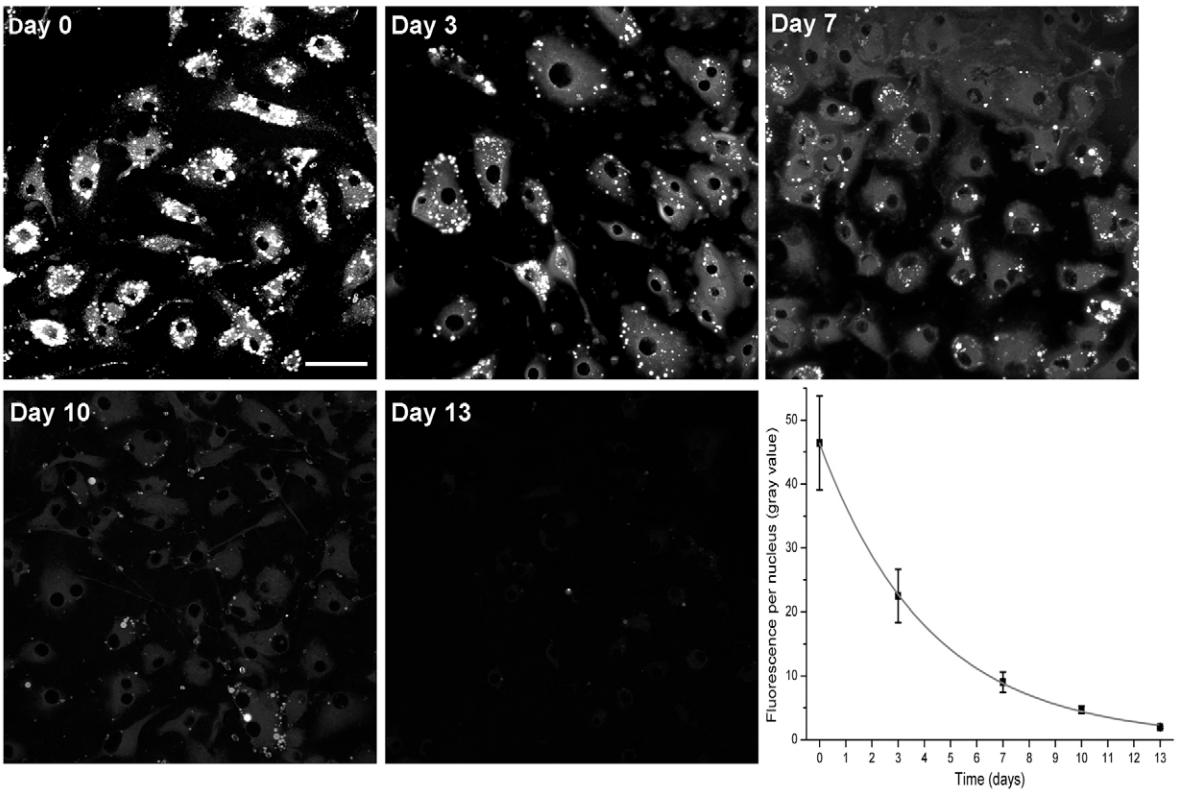

Fig. 4. Loss of coumarin-6 fluorescence from PLGA particles. NPs were internalized for 3 hours, after which confocal images were taken (same imaging settings for all days). Day 0 is 3 hours after adding NPs. After incubating in primary macrophages for 3, 7, 10 and 13 days, new images were recorded. The graph shows quantification of the average fluorescence intensity per cell, i.e. the sum of gray values of all pixels in the image divided by the number of nuclei. The error bars indicate s.e.m. The solid line is the exponential decay fit of the data (fitted lifetime 4.2 days). Scale bar: 50 μm.

coumarin-6 that then diffuses into the cytoplasm and in a further step, out of the cells.

EM analysis of PLGA NPs in macrophages

We next used EM to further substantiate the results from the light microscopy on the intracellular location of NPs. We initially used conventional epoxy resin embedding but found (unsurprisingly) that the solvents used for dehydration completely dissolved the PLGA NPs; and holes in the sections, suggestive of extracted NPs were observed. The use of a shorter protocol involving microwave embedding did not improve the situation (results not shown).

We therefore focused on the use of the Tokuyasu thawed cryo-section method (Griffiths et al., 1993) that avoids the use of chemical solvents. This method also has the advantage that the sections, after thawing, can be immunogold labeled. In one set of experiments, PLGA NPs were internalized into primary macrophages for up to 5 days. We then took advantage of the use of two different-sized gold particles to differentially label early and late endocytic organelles in living cells after the uptake of the PLGA NPs. For this, 15 nm diameter gold-BSA particles were internalized into primary macrophages for 2 hours and followed by a 3 hours chase; under this condition the gold accumulates in lysosomes. Subsequently, the cells were incubated with a high concentration of 5 nm gold-BSA for 5–7 minutes to label (predominantly) early endocytic organelles (Griffiths et al., 1989). Thawed cryo-sections were prepared and labeled with an antibody against LAMP 2 and identified via rabbit anti-mouse followed by 10 nm protein A gold in a three-step labeling procedure. In these sections the localization of PLGA NPs was related to the two markers for lysosomes (15 nm and 10 nm gold) and to the marker for early endosomes (5 nm gold) (Fig. 5A,C,E).

Fig. 5A shows one example from a cell that internalized a PLGA particle whose surrounding membrane is labeled for LAMP 2. In Fig. 5C, from cells with the internalized 15 nm gold particles, both this luminal marker (arrows) and the membrane marker LAMP 2 labeling (arrowheads) were found on the periphery of the PLGA particle. The fluid phase luminal marker of early endosomes (5 nm gold) was clearly separate from the fluid phase luminal marker of lysosomes (15 nm gold) (results not shown; see Fig. 5E, inset). In Fig. 5E also the small PLGA NPs prepared by the selective centrifugation procedure were observed to colocalize with both the 10-nm gold membrane marker (LAMP 2) and the fluid phase luminal marker of lysosomes (15 nm gold). A quantitative analysis indicated that 93% of the NPs in the cells were positive for either LAMP2 or the internalized15 nm gold-BSA (Table 2).

In another set of experiments we related the localization of the PLGA NPs to BCG bacteria (Fig. 5B,D,F). Bacteria were internalized for 3 hours followed by a chase period of 3 hours and, subsequently, the PLGA NPs were internalized for 1 hour followed by a 2-hour chase. Finally, the 15 nm gold BSA was internalized for 2 hours followed by a further 24-hour chase. The

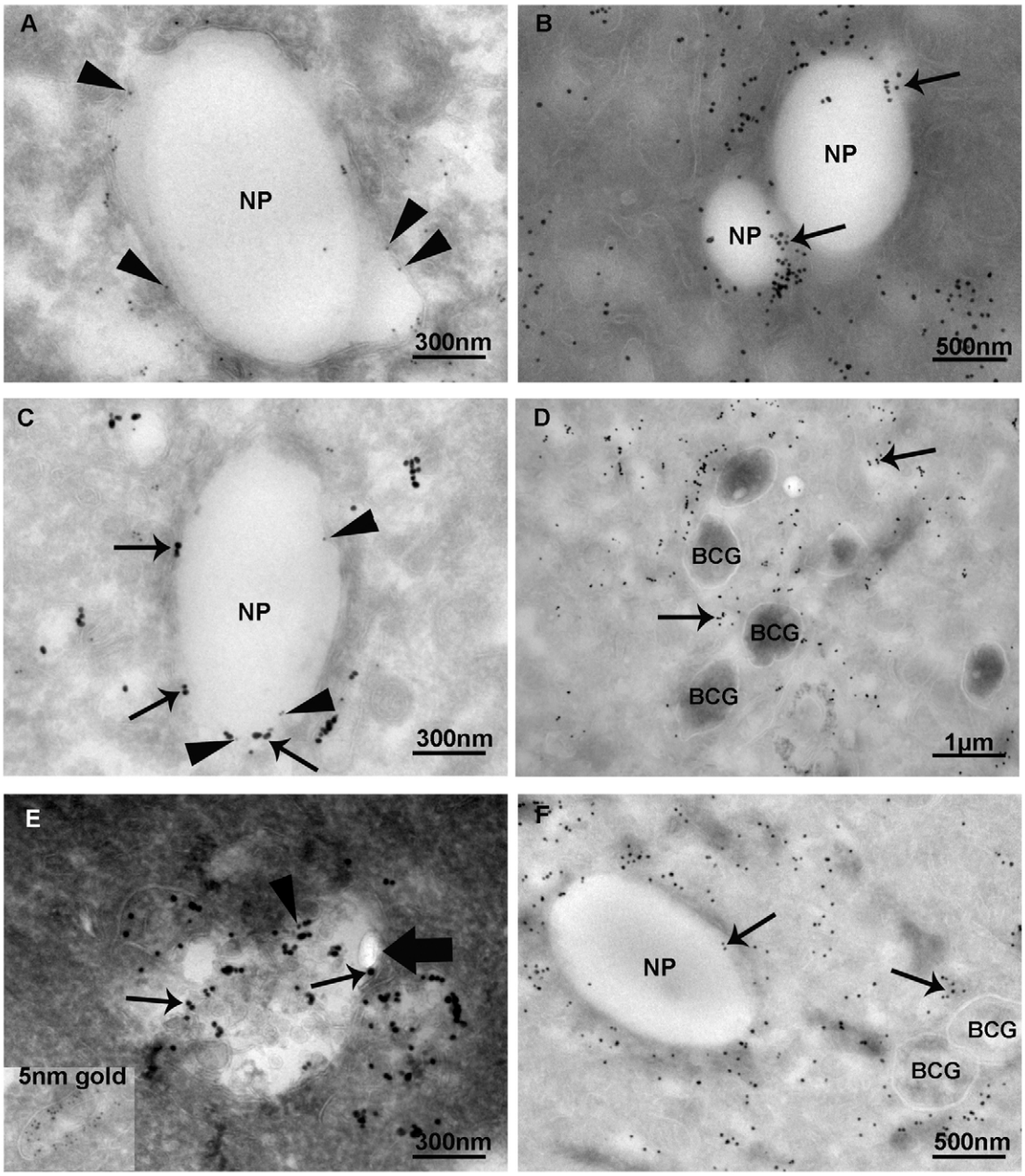

Fig. 5. Localization of PLGA particles and BCG bacteria relative to endosome and lysosomal markers using immuno-EM. (**A**,**C**,**E**) PLGA particles in primary macrophages without bacteria. (**B**,**D**,**F**) PLGA particles from primary macrophages with both NPs and BCG. The endocytic markers used were: 5 nm gold for early endosomal compartment;15 nm gold that was internalized into lysosomes (arrows); and, only on the cells without BCG (A,C,E), 10 nm gold labeling for LAMP 2 (arrowheads) (LAMP 2 labeling could not be done on BCG infected cells because the antibodies cross-react with the bacteria). The NPs were prepared by the standard method, except for E (selective centrifugation). (A) LAMP 2 labeling is apparent on the membrane around the PLGA particle. (C) Both LAMP 2 and 15 nm gold markers are present. (E) Thick arrow indicates a small NP in a vesicle labeled for 15 nm gold and LAMP 2. The inset shows an early endosome from the same preparation that is labeled with the 5 nm gold (early endosome). In the BCG infected cells, the NPs colocalize with 15 nm gold (B,F) while the BCG compartments exclude this marker (D,F).

15 nm gold strongly colocalized with the PLGA NPs (Fig. 5B,F), and both the NPs and the 15 nm gold were clearly distinct from the BCG bacteria (Fig. 5D,F). This result is consistent with the results from the confocal microscopy data (Fig. 2) and it confirms that the PLGA particles are in lysosomes, while the BCG remains segregated into a phagosomal compartment that is inaccessible to lysosomal markers (Fig. 5D,F).

Therapeutic effects of PLGA-rifampicin NPs against BCG in primary macrophages

The final question was to establish whether the NPs that we fabricated enclosing rifampicin had a therapeutic effect against BCG in primary macrophages.

In preliminary experiments we compared three concentrations of PLGA (25, 50 and 100 μg/ml) having varying amounts of

Table 2. NP colocalization with LysoTracker Red and DQ-Red

Day	Lysotracker Red + PLGA Coumarin-6 (%)	DQ-Red + PLGA Coumarin-6 (%)	EM lysosomes (%)
1	100	90.3±1.9	93
4	100	90.2±2.1	N.D.
7	100	92.2±1.3	N.D.

Values indicate the percentage of NPs colocalized with LysoTracker Red and DQ-Red in primary macrophages after 1, 4 and 7 days of incubation, using fluorescence microscopy, and the percentage of NPs in LAMP2-positive compartments after 1 day by immuno-EM. Results represent means ± s.d. of 200 NPs from three independent experiments. N.D., not determined.

rifampicin, as well as NPs without the antibiotic. There were variable effects of the highest concentrations of PLGA, with some, but not all, batches showing high toxicity – with many cells coming off the dishes – suggesting cell death (Results not shown). For the remaining experiments we focused on using 25 and 50 μg/ml PLGA. Fig. 6A shows an experiment in which PLGA NPs encapsulating only 1% rifampicin loading showed little effect on the CFU levels over 15 days, relative to the untreated, infected controls or infected cells treated with NPs lacking the antibiotic. In contrast, NPs having a 31% rifampicin loading led to a total killing of the BCG by 15 days post-infection, with the 50 μg/ml showing a faster rate of killing than the 25 μg/ml NPs (Fig. 6A). Fig. 6B shows the average results from three separate experiments with two different batches of PLGA NPs, having either no rifampicin or loaded at 31% with the antibiotic.

Fig. 6C shows an experiment in which the NPs loaded with rifampicin (at 50 μg/ml) were compared in the same experiment with freely administered rifampicin at 25 or 50 μg/ml, under two conditions: First, the cells were exposed to the antibiotic for only 3 hours, the same time as the exposure of the cells to the NPs. Under this condition therapy is evident, although it is less effective than the NPs. When the antibiotic was left on the cells continuously it was able to clear most of the infection by 1 day and completely by 6 days. It should be noted that it is unlikely that macrophages in the body could maintain such a continuously high concentration of rifampicin. Moreover, since only about one third of the weight of the NPs is antibiotic, the concentration of the free rifampicin used for the treatment is 1.5 times higher for the 25 μg/ml and 3 times higher for the 50 μg/ml.

These experiments show convincingly that, provided there is a sufficient load of antibiotic in the NPs, one dose of these particles releases sufficient rifampicin in the macrophages to completely kill the mycobacteria.

Discussion

At the outset of this study we had two major goals. The first was to resolve the controversial question of whether after uptake into cells the intact NPs escape into the cytoplasm from the phagocytic compartment, or alternatively if they remained in a membrane-enclosed compartment. The second goal was to produce NPs that are able to kill BCG with great efficacy in infected macrophages. In order to achieve these goals we made PLGA NPs containing either coumarin-6 or rifampicin. We managed to fabricate NPs enclosing sufficient coumarin-6 to make the particles fluorescent and up to 10% loading of rifampicin; however this concentration of antibiotic was too low to achieve sufficient killing of BCG. So for the rest of the study we used coumatin-6 NPs for the light microscopy localization analyses and, separately, we focused on achieving sufficient rifampicin by itself in PLGA NPs.

The localization of PLGA NPs has been disputed widely in the literature in the past 10 years (see Introduction). In order to clarify this issue we decided to use a combination of different techniques to achieve a better understanding of where PLGA NPs reside. Our study shows unequivocally that in our system PLGA nanoparticles, irrespective of size, once internalized by primary and RAW macrophages, remain for at least one week in phago-lysosomes. Using confocal microscopy we found that NPs colocalize with LysoTracker Red, DQ-Red BSA and LAMP-2. A further confirmation came from electron microscopy where 93% of NPs colocalized with lysosomal, but not early endosomal markers.

Once we evaluated NP localization in macrophages we were interested in understanding whether this would change in the presence of BCG bacteria. Our data show that when either mouse primary macrophages or RAW cells were infected with red BCG and allowed to internalize the coumarin-6 green-labeled particles, there was no evident colocalization between the bacteria and the PLGA particles. This result is in agreement with the conclusions made by (Kisich et al., 2007), but at odds with the findings of (de Faria et al., 2012) who concluded that PLGA NPs enclosing an isoniazid derivative directly interacts with the BCG phagosomes in macrophages. Earlier studies had established that BCG, like M.tb, resides in an arrested early phagosome stage, with only a small fraction of phagosomes acquiring markers of lysosomes. In contrast, the NPs added to the cells after the bacteria, bypass the bacterial compartments and transport more distally into the macrophages into a low pH, hydrolase-rich, late phago-lysosome stage.

Collectively, our data support the conclusions of (Schliehe et al., 2011) who found that larger PLGA MPs remained in LAMP 1-positive lysosomes in dendritic cells and macrophages for at least two days after phagocytosis. They provided indirect evidence that ovalbumin encapsulated in the MPs was able to enter the cytoplasm of these cells and could activate the endoplasmic reticulum based MHC-1 pathway of antigen presentation to CD8+ T cells (‘cross-presentation’). Many other groups had shown similar cross-presentation data from encapsulated protein antigens, or DNA in PLGA NPs or MPs (Audran et al., 2003; Nixon et al., 1996; Partidos et al., 1999). From such data it had been concluded by many that, rather than the antigen, it is the intact PLGA particles that lyse the phagosomal/endosomal membrane and subsequently release the antigen into the cytoplasm (Shen et al., 2006). Such an interpretation would be in agreement with the papers by Panyam and collaborators, who saw accumulation of coumarin-6 from NPs in the cytoplasm (Panyam et al., 2002). Even though our data disagree fundamentally with that interpretation, at least in mouse primary, and RAW macrophages, the issue of how peptide antigens, or encapsulated DNA cross the membranes of the compartments in the endocytic pathway remains an open question. We assume that hydrophobic, uncharged molecules such as coumarin-6 and rifampicin easily cross membranes by diffusion and this would explain how sufficient antibiotic is able to cross two membranes. The first is the phago-lysosome membrane enclosing the NP (phagosome to cytoplasm) and the second is the membrane of the phagosome enclosing the BCG

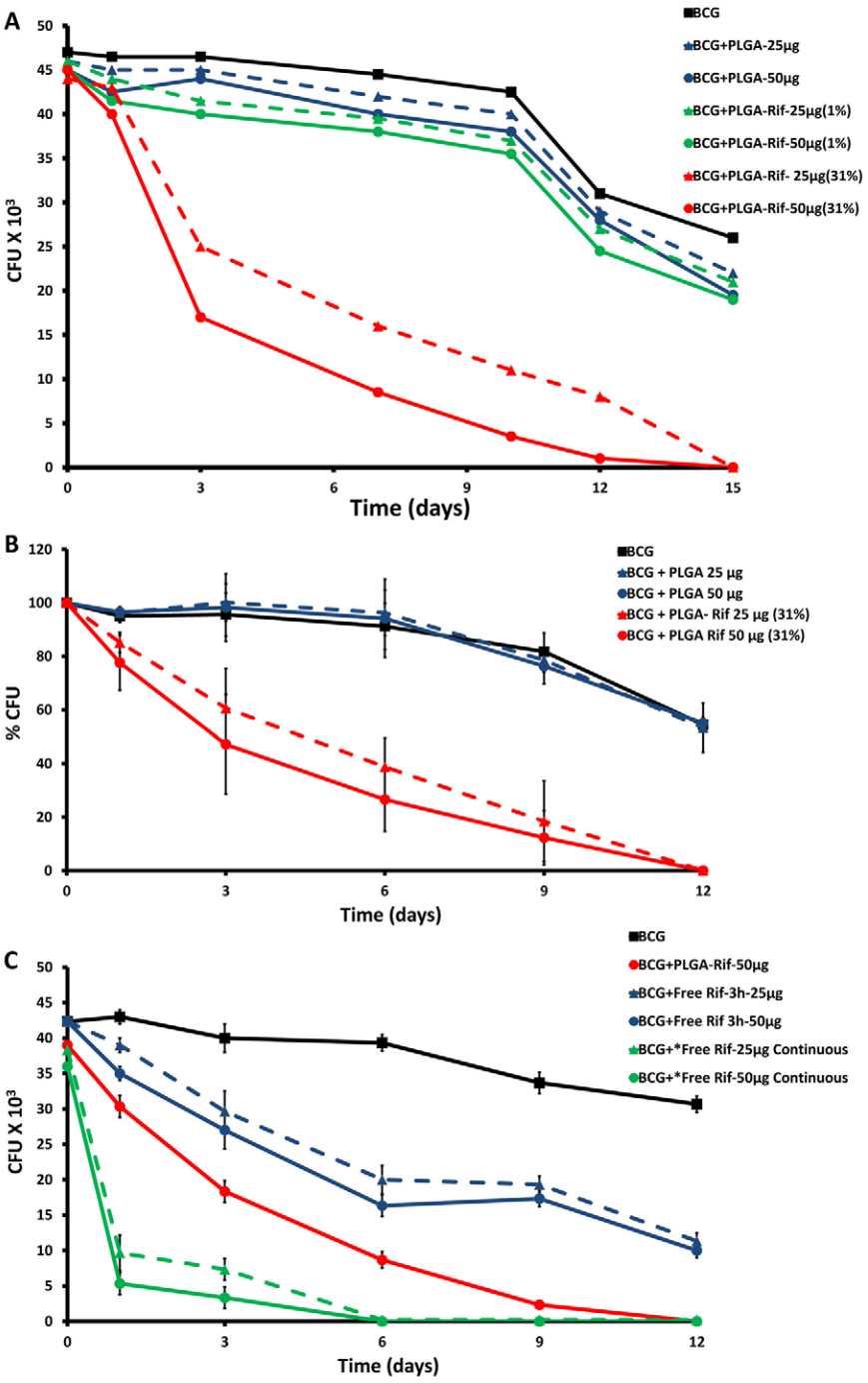

Fig. 6. Effects of PLGA-rifampicin in killing BCG in primary macrophages. Experiments in which primary macrophages were infected with BCG either without further treatment (BCG) or treated with different batches of PLGA NPs (with either 1% or 31% rifampicin loading) at either 25 or 50 µg/ml. (**A**,**B**) In (A) are shown results of two independent measurements of CFU. (B) The mean ± s.d of three independent experiments are shown. (**C**) The effect of rifampicin NPs (3 hour treatment) is compared directly with that of free rifampicin (25 or 50 µg/ml) given for either 3 hours only or continuously on the cells for the whole experiment (with fresh antibiotic added every 3 days).

(cytoplasm to phagosome), as suggested by (Hirota et al., 2010). The experiment in Fig. 4 and supplementary material Fig. S3 is consistent with the first part of this hypothesis (phagosome to cytoplasm).

One relevant issue of this finding from the point of view of therapy, is that the compartment where the rifampicin is released is spatially separated from the compartment where the mycobacteria are localized. It seems logical to ask whether the therapy would be more efficient if the NPs could be selectively targeted to the mycobacterial phagosome by the addition of NPs surface ligands, such as mannose or IgG, that bind to specific receptors on the macrophage plasma membrane. In one study enhanced therapy against M.tb in the guinea pig system was seen with PLGA NPs conjugated with the lectin wheat germ agglutinin, relative to unconjugated NPs, after both oral and aerosol administration (Sharma et al., 2004b). Whether the lectin facilitated NPs crossing epithelial barriers, or uptake into macrophages, or both, remains to be elucidated.

Provided sufficient rifampicin was loaded into our PLGA NPs, we consistently found that a single dose given after infection could efficiently kill all detectable BCG in primary macrophages within 8–12 days, as determined by CFU analysis (Fig. 6). However, preparations with 1–5% rifampicin encapsulation in NPs led to insignificant killing (Fig. 6A; data not shown). The

efficiency of BCG killing (100%) that we saw with NPs having a loading efficiency of 31% rifampicin exceeded the efficiency observed in earlier studies in the rat alveolar macrophage cell line (NR8383) after 7 days (Hirota et al., 2010) or 14 days infection (Yoshida et al., 2006). As shown in Fig. 6C when free rifampicin was administered for the same time as the rifampicin NPs it was less effective than the NPs. This agrees with many earlier studies with both BCG and M.tb in macrophages (Barrow et al., 1998; Hirota et al., 2010; Kisich et al., 2007; Quenelle et al., 2001; Yoshida et al., 2006) and in many mammalian models of M.tb (Griffiths et al., 2010).

In summary, our PLGA NPs encapsulating rifampicin and coumarin-6, given as a single 3 hours dose after infection with BCG, remains inside phago-lysosomes separated from the BCG phagosomes and when PLGA-rifampicin is used, sufficient antibiotic is released into the infected cell cytoplasm over a 12 day period to efficiently clear the infection.

Materials and Methods

Chemicals

PLGA, poly(D,L-lactide-co-glycolide), 50:50 RESOMER® RG 502 was bought from Evonik Röhm Gmbh, Polyvinyl alcohol (PVA) 86–89% (molecular weight 57,000–66,000) was bought from Alfa Aesar. Rifampicin was bought from Sigma and Coumarin-6 from Aldrich. Lysotracker Red DND 99 and DQ-Red BSA was purchased from Molecular probes. Recombinant mouse macrophage colony stimulating factor (rm M-CSF) was bought from Immunotools GmbH Germany. Rat anti mouse LAMP2 was purchased from Iowa Hybridoma bank. Rabbit anti mouse conjugated to Alexa 594 was bought from Molecular probes. Rat anti mouse CD 14 was from BD biosciences.

Nanoparticle preparation

Method A: Standard oil in water emulsion

To encapsulate rifampicin, an oil-in-water emulsion (O/W) using the solvent evaporation method was used as our standard procedure to prepare rifampicin loaded nanoparticles. Rifampicin (100 mg) and PLGA (100 mg) were dissolved in 10 ml dichloromethane, with or without 0.2 mg of coumarin-6 and stirred overnight at room temperature. For the water phase 200 mg of PVA was dissolved in 20 ml water (pre-filtered using a 0.2 μm filter) with heating to 90 degrees for 1 hour and stirring vigorously with a magnetic stirrer overnight at room temperature. The two solutions were mixed and tip-sonicated (Sonics, Vibracell) for 3 minutes to obtain the primary emulsion. Subsequently, the emulsion was put in a flask and kept stirring, allowing complete evaporation of the DCM within 10–14 hours. For this, a piece of aluminum foil was applied on the top of the flask and punctured with a hole of about 0.5 cm diameter. Once the evaporation step was completed, NPs were washed twice with water and collected via centrifugation at 8000 r.p.m. for 20 minutes using a Beckman coulter 32 Ti rotor. Subsequently, they were re-suspended in a 0.5% mannitol solution (Ohashi et al., 2009), freeze-dried for 2 days and stored at 4℃.

Method B: Small uniform beads using selective centrifugation

In order to obtain smaller, more uniform nanoparticles than the standard method (above) we used the method described by (Gaumet et al., 2007). After evaporation the NPs were washed twice with water and, after re-suspension, they were selectively centrifuged using different relative centrifuge forces (RCF). For this, we used a Beckman L-80 Ultracentrifuge and a rotor Beckman coulter SW 32 Ti. First we applied a RCF of 167, then one of 4000 and finally one of 30,000, in each case for 120 minutes. NPs collected at 30,000 RCF were freeze-dried (as above) and evaluated for size using transmission electron microscopy (TEM) and scanning electron microscopy (SEM).

In vitro rifampicin release from NPs

Rifampicin loaded NPs (1 mg/ml) were incubated at 37℃ in HEPES buffer (100 mM pH 7,4) or acetate buffer (pH 4). The amount of rifampicin was estimated every day for 12 days by spectrophotometry at 475 nm. At each time point NPs were pelleted by centrifugation (13,000 ***g*** for 5 minutes) and the all of the supernatant was removed and measured, then fresh buffer was added to the NPs.

Nanoparticle microscopy

Negative staining TEM

1 mg of dried NPs was dissolved in MQ water and subsequently bath-sonicated for 1 minute. The material was negatively stained with 3% uranyl acetate (in H_2O) and imaged at 80 kV using a Philips CM200 TEM.

SEM

The NPs in the form of dried powder was mounted on the specimen stab and coated with a thin film of gold via sputtering. The samples were analyzed with a Hitachi S-4800 SEM.

Cryo-TEM

The samples were prepared by placing 5 μl nanobead dispersion on copper grids having a holey carbon film and blotted with filter paper. The grids were vitrified in liquid ethane. A Gatan cryo-holder was used to transfer grids into the Philips CM200 EM. The images were recorded digitally with a CCD camera under low electron dose conditions.

Fluorescence microscopy

1 μl of the NP suspension was placed on a glass slide, covered with a coverslip and subsequently analyzed at 100× on a Leica DM IRBE fluorescence microscope.

Zeta potential measurements

Zeta potential experiments were conducted with the aid of a Zeta-sizer Nano ZS, MAL1049741 (Malvern instruments Ltd, U.K) in automatic mode. Plastic cuvettes and the dip cell type 1 including palladium electrodes with 2 mm spacing were used. The values of the electrophoretic mobility of the nanoparticles in the suspension were converted to zeta potential values. The measurements were carried out at 25℃ in 0.15 M NaCl to mimic physiological conditions.

Dynamic light scattering

NPs were suspended in pure milli-MQ water and filtered in an atmosphere of filtered air through a 5 μm filter (Millipore) directly into pre-cleaned 10 mm NMR tubes. The experiments were performed at 25℃ by means of an ALV/CGS-8F multi-detector version compact goniometer system, with eight fiber-optical detection units (ALV-GmbH, Langen, Germany). The intensity correlation function was measured at eight scattering angles simultaneously in the range 22–14° with four ALV5000/E digital correlators.

HPLC-UV

Samples (1–2 mg) were dissolved in 1 ml acetonitrile (ACN HiPerSolv Chromanorm, VWR, Radnor, PE, US) with Ultra sonication for 10 minutes. The samples were centrifuged (13,000 ***g***, 1 minute) and 0.5 μl of the supernatant was injected by an Agilent 1200 series GL1377A micro WPS auto sampler. When necessary, the samples were diluted ten times before injection. Rifampicin and coumarin-6 were separated with an ACE3 C18 column (150×0.3 mm inner diameter; Advanced Chromatography Technologies, Aberdeen, UK). An Agilent 1100 series GL1378 pump (Agilent technologies, Palo Alto, CA, USA) was used to deliver a mobile phase consisting of ACN/Type 1 water/formic acid (75/24.9/0.1, v/v/v%). The analytes were detected using an Agilent 1200 series GL1365D MWD detector (254 nm).

Bacterial culture

M. bovis BCG-DS Red were grown on Middlebrook's 7H9 broth medium (Difco) supplemented with 10% OADC (V/V), glycerol 0.02% and 0.05% of Tween 80 v/v until exponential phase at 37℃ incubator without agitation. For some experiments we also used GFP-BCG.

Raw 264.7 macrophage culture

The mouse macrophage cell line was cultured in RPMI 1640 supplemented with 10% FCS, 1% penicillin/streptomycin and glutamine (25 mM). For plating, the cells were washed twice with PBS, scraped with cell scraper and incubated in 5% CO_2 incubator at 37℃.

Bone marrow-derived macrophage isolation and culture

Experiments were performed with 6- to 8-week-old C57BL/6 male or female mice from the University of Oslo (IBV) animal facility. All animal experiments were performed according to the relevant regulatory standards. Mice were killed by cervical dislocation and the femur and tibia bones were dissected. The bones were trimmed at both ends and the marrow was flushed out with 5 ml of RPMI containing 10% FCS using a 25-gauge needle. The cell suspension was centrifuged for 5 minutes at 1500 ***g*** and the pellet was gently re-suspended in RPMI supplemented with 10% FCS, 1% penicillin/streptomycin, glutamine 25 mM, and M-CSF 40 ng/ml and plated into Petri dishes. After 3 days, 50% of the medium was changed, the cells were incubated for 2 days and then washed with 1% FCS in PBS, and again incubated for another day. At this point, more than 95% of cells were routinely positive for the macrophage surface marker CD14, as assessed by immunofluorescence microscopy. Cells were scraped and plated in 12-well plates at a density of 5×10^5 cells/ml and incubated over night before infection.

Primary macrophages infected with *M. bovis* DS-Red BCG and treated with PLGA nanobeads

Primary macrophages were seeded in 12-well plates at a density of 5×10^5 cells per 0.5 ml per well and incubated overnight in a 5% CO_2 incubator. DS-Red BCG were pelleted in the exponential grown phase, washed twice in PBS pH 7.4, and re-suspended in serum-free RPMI medium to a final concentration of $5–8\times10^9$ cells/ml. A 10-minute pulse in a water-bath sonicator was followed by passage through a 23-gauge needle to disrupt bacterial clumps. Before infection, residual bacterial aggregates were removed by low-speed centrifugation (120 ***g***) for 2 minutes. Single-bacteria suspension was verified by fluorescence microscopy. Infection proceeded with BCG in the ratio of 1:10 bacteria per macrophage, to achieve about 1–10 bacteria inside macrophages after 3 hours uptake. The cells were washed twice with PBS to remove extracellular bacteria. After a 2-hour chase in medium without bacteria, PLGA NPs were added to the cells at 25 µg, 50 µg and (in initial experiments only) 100 µg to each well – a total volume of 1 ml per well. After 3 hours of incubation, cells were washed with PBS to remove extracellular particles. After specified time periods macrophages were lysed using distilled water containing 0.005% SDS. Serial dilutions of the lysates were prepared in PBS and plated on Middlebrook 7H10 medium supplemented agar with OADC. After about 2–3 weeks of incubation at 37℃, colonies were counted.

Free rifampicin was administered from a stock solution (10 mg/ml in 20% DMSO in water.) This was dissolved in RPMI medium to give a final concentration of 25 or 50 µg/ml and administered either as one 3-hour dose or continuously for the whole experiment, with the antibiotic being replaced freshly every 3 days.

Localization of biodegradable PLGA nanobeads in live-cell primary and RAW macrophage using LysoTracker Red and DQ-Red BSA

LysoTracker Red DND 99 was diluted with RPMI imaging medium to a 1:2000 dilution ratio to give 75 nM final concentration. This was added to the PLGA coumarin-6, with or without rifampicin-treated macrophages and incubated for 5 minutes in a 37℃ 5% CO_2 incubator before washing with RPMI medium. Then the cells were imaged live without fixing, using an inverted Olympus IX81 FV1000 confocal microscope. The same procedure was followed when using DQ-Red BSA staining (10 µg/ml) for RAW cells and 20 µg/ml for primary macrophages. The DQ-Red BSA was incubated with the live cells for 30 minutes at 37℃.

Quantification of coumarin-6 fluorescence loss from NPs in primary macrophages

NPs containing coumarin-6 were internalized for 3 hours into primary macrophages (without bacteria). After washing the cells to remove external NPs the cells were incubated for a further 13 days. At selected times, the cells were fixed in paraformaldehyde (as above) and imaged using confocal microscopy (Olympus Fluoview-1000, 40× objective), using identical imaging settings for each time point. The total fluorescence signal per image (sum of gray values of all pixels) was divided by the number of cell nuclei, to give the average fluorescent signal per cell. In addition, the fluorescence intensity of coumarin-6 in the cytoplasm (i.e. areas in the cell free from NPs) was determined by taking the average gray value average for ten different cytoplasmic regions selected as being free of NPs, for each time point (using ImageJ) giving the cytoplasmic coumarin-6 level over time.

Immunofluorescence microscopy

Macrophages treated with PLGA coumarin-6 NPs, as described above, were fixed with freshly prepared 4% paraformaldehyde PBS for 15 minutes at room temperature and washed three times with PBS. Subsequently, the cells were permeabilized with 0.05% saponin and 0.2% BSA in PBS for 5–10 minutes. The cells were washed with PBS and blocked with BSA (1% w/v PBS) for 15 minutes before incubation with rat anti mouse LAMP-2 primary antibody (in BSA/PBS) that was detected with rabbit anti mouse-Alexa Fluor 594 antibody. The coverslips were mounted on glass slides with Moviol.

Localization of PLGA NPs in primary macrophages using electron microscopy

For these experiments we used two conditions: (1) Primary macrophages having internalized PLGA NPs were pulsed (2 hours) with 15 nm gold-BSA and then chased (3 hours) in live cells. Under these conditions the gold is exclusively localized into late endosomes and lysosomes (abbreviated for simplicity as 'lysosomes') (Griffiths et al., 1988; Griffiths et al., 1990). Just prior to fixation, the cells were incubated with 5 nm gold-BSA for 5–7 minutes to label early endosomes followed by fixation for 24 hours with paraformaldehyde (4% w/v in 200 mM HEPES buffer pH 7.4). (2) In a different set of primary macrophages, the cells were infected with BCG (as above) for 2 hours followed by a 1–2 day chase, then incubated with NPs as above. The cells were then incubated with the 15 nm gold-BSAs as above.

Cells were fixed with paraformaldehyde (4% w/v in 200 mM HEPES pH 7.4 buffer) for 24 hours at room temperature. The sample was then washed in the same buffer and the cells were scraped and centrifuged to obtain a pellet. Pieces of the pellet were embedded in 10% gelatin and cryo sectioned as described (Griffiths et al., 1993; Tokuyasu, 1978). The sections were picked up with a 50:50 solution of 2% methyl cellulose and 2.3 M sucrose (Liou et al., 1996). The sections were labeled with LAMP-2 antibody, that was detected using rat anti-mouse followed by protein A gold (10 nm) then embedded in 2% methyl cellulose, 3% uranyl acetate (ratio 8:2) and visualized in the TEM.

Acknowledgements

We thank Nathalie Winter and Brigitte Gicquel for the DS-Red BCG and Michael Niederweis for the BCG GFP. We thank Anna-Lena Kjøniksen and Shirin Fanaian for help with the DLS and zetasizer estimates. We greatly appreciate the support of Tove Bakar for her general support with the EM and Antje Hoenen for helping with the SEM imaging. We also appreciate the support of Hilde Hyldmo from the IMBV animal facility. The help of Eik Hoffmann with the methods to isolate and maintain the primary macrophages is greatly appreciated. The authors also appreciate the use and support by the NORMIC-UiO imaging platform at the Department of Molecular Biosciences, University of Oslo. We thank Maximilliano Gutierrez and Jon Hildahl for critically reading the paper. D.W. would like to thank for the MRC Laboratory for Molecular Biology and Beatrice Lowe for their funding and support. The authors declare no competing interests.

Author contributions

R.K. carried out the macrophage infection experiments, and R.K. and D.W. did the light microscopical analyses. D.W. and G.K. carried out the quantitative fluorescence analyses. F.F. made the EM analyses, with N.R., and the nano particles, with help from L.U., A.M., M.P.M., A.S., G.K.K. and B.N. W.E.-J., H.R.-L. and S.W. carried out the HPLC analyses of the drug content of NPs. The project was coordinated by G.G., who wrote the paper in conjunction with R.K., F.F. and D.W.

Funding

This work was supported in part by PhD funding from the University of Oslo (UiO) Molecular Life Sciences to F.F., by the IBV to R.K. and the UiO MatNat Faculty to L.U.

Supplementary material available online at
http://jcs.biologists.org/lookup/suppl/doi:10.1242/jcs.121814/-/DC1

References

Anisimova, Y. V., Gelperina, S. I., Peloquin, C. A. and Heifets, L. B. (2000). Nanoparticles as Antituberculosis drugs carriers: effect on activity against mycobacterium tuberculosis in human monocyte-derived macrophages. *J. Nanopart. Res.* **2**, 165-171.

Audran, R., Peter, K., Dannull, J., Men, Y., Scandella, E., Groettrup, M., Gander, B. and Corradin, G. (2003). Encapsulation of peptides in biodegradable microspheres prolongs their MHC class-I presentation by dendritic cells and macrophages in vitro. *Vaccine* **21**, 1250-1255.

Barrow, E. L., Winchester, G. A., Staas, J. K., Quenelle, D. C. and Barrow, W. W. (1998). Use of microsphere technology for targeted delivery of rifampin to Mycobacterium tuberculosis-infected macrophages. *Antimicrob. Agents Chemother.* **42**, 2682-2689.

Cartiera, M. S., Johnson, K. M., Rajendran, V., Caplan, M. J. and Saltzman, W. M. (2009). The uptake and intracellular fate of PLGA nanoparticles in epithelial cells. *Biomaterials* **30**, 2790-2798.

Cheng, F. Y., Wang, S. P., Su, C. H., Tsai, T. L., Wu, P. C., Shieh, D. B., Chen, J. H., Hsieh, P. C. and Yeh, C. S. (2008). Stabilizer-free poly(lactide-co-glycolide) nanoparticles for multimodal biomedical probes. *Biomaterials* **29**, 2104-2112.

Couvreur, P. and Vauthier, C. (2006). Nanotechnology: intelligent design to treat complex disease. *Pharm. Res.* **23**, 1417-1450.

Danhier, F., Ansorena, E., Silva, J. M., Coco, R., Le Breton, A. and Préat, V. (2012). PLGA-based nanoparticles: an overview of biomedical applications. *J. Control. Release* **161**, 505-522.

Davis, M. E., Chen, Z. G. and Shin, D. M. (2008). Nanoparticle therapeutics: an emerging treatment modality for cancer. *Nat. Rev. Drug Discov.* **7**, 771-782.

de Faria, T. J., Roman, M., de Souza, N. M., De Vecchi, R., de Assis, J. V., dos Santos, A. L., Bechtold, I. H., Winter, N., Soares, M. J., Silva, L. P. et al. (2012). An isoniazid analogue promotes Mycobacterium tuberculosis-nanoparticle interactions and enhances bacterial killing by macrophages. *Antimicrob. Agents Chemother.* **56**, 2259-2267.

Desjardins, M. and Griffiths, G. (2003). Phagocytosis: latex leads the way. *Curr. Opin. Cell Biol.* **15**, 498-503.

Dye, C. and Williams, B. G. (2010). The population dynamics and control of tuberculosis. *Science* **328**, 856-861.

Gaumet, M., Gurny, R. and Delie, F. (2007). Fluorescent biodegradable PLGA particles with narrow size distributions: preparation by means of selective centrifugation. *Int. J. Pharm.* **342**, 222-230.

Gomes, A. J., Faustino, A. S., Machado, A. E., Zaniquelli, M. E., de Paula Rigoletto, T., Lunardi, C. N. and Lunardi, L. O. (2006). Characterization of PLGA microparticles as a drug carrier for 3-ethoxycarbonyl-2h-benzofuro[3,2-f]-1-benzopyran-2-one. Ultrastructural study of cellular uptake and intracellular distribution. *Drug Deliv.* **13**, 447-454.

Griffiths, G., Hoflack, B., Simons, K., Mellman, I. and Kornfeld, S. (1988). The mannose 6-phosphate receptor and the biogenesis of lysosomes. *Cell* **52**, 329-341.

Griffiths, G., Back, R. and Marsh, M. (1989). A quantitative analysis of the endocytic pathway in baby hamster kidney cells. *J. Cell Biol.* **109**, 2703-2720.

Griffiths, G., Matteoni, R., Back, R. and Hoflack, B. (1990). Characterization of the cation-independent mannose 6-phosphate receptor-enriched prelysosomal compartment in NRK cells. *J. Cell Sci.* **95**, 441-461.

Griffiths, G., Burke, B. and Lucocq, J. (1993). *Fine Structure Immunocytochemistry*. Berlin/New York, NY: Springer-Verlag.

Griffiths, G., Nyström, B., Sable, S. B. and Khuller, G. K. (2010). Nanobead-based interventions for the treatment and prevention of tuberculosis. *Nat. Rev. Microbiol.* **8**, 827-834.

Hirota, K., Hasegawa, T., Nakajima, T., Inagawa, H., Kohchi, C., Soma, G., Makino, K. and Terada, H. (2010). Delivery of rifampicin-PLGA microspheres into alveolar macrophages is promising for treatment of tuberculosis. *J. Control. Release* **142**, 339-346.

Hussain, N., Jaitley, V. and Florence, A. T. (2001). Recent advances in the understanding of uptake of microparticulates across the gastrointestinal lymphatics. *Adv. Drug Deliv. Rev.* **50**, 107-142.

Jain, S. K., Gupta, Y., Ramalingam, L., Jain, A., Jain, A., Khare, P. and Bhargava, D. (2010). Lactose-conjugated PLGA nanoparticles for enhanced delivery of rifampicin to the lung for effective treatment of pulmonary tuberculosis. *PDA J. Pharm. Sci. Technol.* **64**, 278-287.

Kjøniksen, A. L., Joabsson, F., Thuresson, K. and Nystrom, B. (1999). Salt-induced aggregation of polystyrene latex particles in aqueous solutions of a hydrophobically modified nonionic cellulose derivative and its unmodified analogue. *J. Phys. Chem. B* **103**, 9818-9825.

Jordao, L., Bleck, C. K., Mayorga, L., Griffiths, G. and Anes, E. (2008). On the killing of mycobacteria by macrophages. *Cell. Microbiol.* **10**, 529-548.

Kisich, K. O., Gelperina, S., Higgins, M. P., Wilson, S., Shipulo, E., Oganesyan, E. and Heifets, L. (2007). Encapsulation of moxifloxacin within poly(butyl cyanoacrylate) nanoparticles enhances efficacy against intracellular Mycobacterium tuberculosis. *Int. J. Pharm.* **345**, 154-162.

Liou, W., Geuze, H. J. and Slot, J. W. (1996). Improving structural integrity of cryosections for immunogold labeling. *Histochem. Cell Biol.* **106**, 41-58.

Makadia, H. K. and Siegel, S. J. (2011). Poly lactic-co-glycolic acid (PLGA) as biodegradable controlled drug delivery carrier. *Polymers* **3**, 1377-1397.

Makino, K., Nakajima, T., Shikamura, M., Ito, F., Ando, S., Kochi, C., Inagawa, H., Soma, G. and Terada, H. (2004). Efficient intracellular delivery of rifampicin to alveolar macrophages using rifampicin-loaded PLGA microspheres: effects of molecular weight and composition of PLGA on release of rifampicin. *Colloids Surf. B Biointerfaces* **36**, 35-42.

Mathiowitz, E., Jacob, J. S., Jong, Y. S., Carino, G. P., Chickering, D. E., Chaturvedi, P., Santos, C. A., Vijayaraghavan, K., Montgomery, S., Bassett, M. et al. (1997). Biologically erodable microspheres as potential oral drug delivery systems. *Nature* **386**, 410-414.

Muttil, P., Kaur, J., Kumar, K., Yadav, A. B., Sharma, R. and Misra, A. (2007). Inhalable microparticles containing large payload of anti-tuberculosis drugs. *Eur. J. Pharm. Sci.* **32**, 140-150.

Nixon, D. F., Hioe, C., Chen, P. D., Bian, Z., Kuebler, P., Li, M. L., Qiu, H., Li, X. M., Singh, M., Richardson, J. et al. (1996). Synthetic peptides entrapped in microparticles can elicit cytotoxic T cell activity. *Vaccine* **14**, 1523-1530.

Ohashi, K., Kabasawa, T., Ozeki, T. and Okada, H. (2009). One-step preparation of rifampicin/poly(lactic-co-glycolic acid) nanoparticle-containing mannitol microspheres using a four-fluid nozzle spray drier for inhalation therapy of tuberculosis. *J. Control. Release* **135**, 19-24.

Onoshita, T., Shimizu, Y., Yamaya, N., Miyazaki, M., Yokoyama, M., Fujiwara, N., Nakajima, T., Makino, K., Terada, H. and Haga, M. (2010). The behavior of PLGA microspheres containing rifampicin in alveolar macrophages. *Colloids Surf. B Biointerfaces* **76**, 151-157.

Pandey, R. and Khuller, G. K. (2004). Chemotherapeutic potential of alginate-chitosan microspheres as anti-tubercular drug carriers. *J. Antimicrob. Chemother.* **53**, 635-640.

Pandey, R. and Khuller, G. K. (2006). Nanotechnology based drug delivery system(s) for the management of tuberculosis. *Indian J. Exp. Biol.* **44**, 357-366.

Pandey, R., Sharma, A., Zahoor, A., Sharma, S., Khuller, G. K. and Prasad, B. (2003). Poly (DL-lactide-co-glycolide) nanoparticle-based inhalable sustained drug delivery system for experimental tuberculosis. *J. Antimicrob. Chemother.* **52**, 981-986.

Panyam, J. and Labhasetwar, V. (2003a). Biodegradable nanoparticles for drug and gene delivery to cells and tissue. *Adv. Drug Deliv. Rev.* **55**, 329-347.

Panyam, J. and Labhasetwar, V. (2003b). Dynamics of endocytosis and exocytosis of poly(D,L-lactide-co-glycolide) nanoparticles in vascular smooth muscle cells. *Pharm. Res.* **20**, 212-220.

Panyam, J., Zhou, W. Z., Prabha, S., Sahoo, S. K. and Labhasetwar, V. (2002). Rapid endo-lysosomal escape of poly(DL-lactide-co-glycolide) nanoparticles: implications for drug and gene delivery. *FASEB J.* **16**, 1217-1226.

Panyam, J., Sahoo, S. K., Prabha, S., Bargar, T. and Labhasetwar, V. (2003). Fluorescence and electron microscopy probes for cellular and tissue uptake of poly(D,L-lactide-co-glycolide) nanoparticles. *Int. J. Pharm.* **262**, 1-11.

Partidos, C. D., Vohra, P., Jones, D. H., Farrar, G. and Steward, M. W. (1999). Induction of cytotoxic T-cell responses following oral immunization with synthetic peptides encapsulated in PLG microparticles. *J. Control. Release* **62**, 325-332.

Quenelle, D. C., Winchester, G. A., Staas, J. K., Barrow, E. L. and Barrow, W. W. (2001). Treatment of tuberculosis using a combination of sustained-release rifampin-loaded microspheres and oral dosing with isoniazid. *Antimicrob. Agents Chemother.* **45**, 1637-1644.

Rohde, K., Yates, R. M., Purdy, G. E. and Russell, D. G. (2007). Mycobacterium tuberculosis and the environment within the phagosome. *Immunol. Rev.* **219**, 37-54.

Schliehe, C., Schliehe, C., Thiry, M., Tromsdorf, U. I., Hentschel, J., Weller, H. and Groettrup, M. (2011). Microencapsulation of inorganic nanocrystals into PLGA microsphere vaccines enables their intracellular localization in dendritic cells by electron and fluorescence microscopy. *J. Control. Release* **151**, 278-285.

Sharma, R., Saxena, D., Dwivedi, A. K. and Misra, A. (2001). Inhalable microparticles containing drug combinations to target alveolar macrophages for treatment of pulmonary tuberculosis. *Pharm. Res.* **18**, 1405-1410.

Sharma, A., Pandey, R., Sharma, S. and Khuller, G. K. (2004a). Chemotherapeutic efficacy of poly(DL-lactide-co-glycolide) nanoparticle encapsulated antitubercular drugs at sub-therapeutic dose against experimental tuberculosis. *Int. J. Antimicrob. Agents* **24**, 599-604.

Sharma, A., Sharma, S. and Khuller, G. K. (2004b). Lectin-functionalized poly(lactide-co-glycolide) nanoparticles as oral/aerosolized antitubercular drug carriers for treatment of tuberculosis. *J. Antimicrob. Chemother.* **54**, 761-766.

Sharma, R., Muttil, P., Yadav, A. B., Rath, S. K., Bajpai, V. K., Mani, U. and Misra, A. (2007). Uptake of inhalable microparticles affects defence responses of macrophages infected with Mycobacterium tuberculosis H37Ra. *J. Antimicrob. Chemother.* **59**, 499-506.

Shen, H., Ackerman, A. L., Cody, V., Giodini, A., Hinson, E. R., Cresswell, P., Edelson, R. L., Saltzman, W. M. and Hanlon, D. J. (2006). Enhanced and prolonged cross-presentation following endosomal escape of exogenous antigens encapsulated in biodegradable nanoparticles. *Immunology* **117**, 78-88.

Sosnik, A., Carcaboso, A. M., Glisoni, R. J., Moretton, M. A. and Chiappetta, D. A. (2010). New old challenges in tuberculosis: potentially effective nanotechnologies in drug delivery. *Adv. Drug Deliv. Rev.* **62**, 547-559.

Tokuyasu, K. T. (1978). A study of positive staining of ultrathin frozen sections. *J. Ultrastruct. Res.* **63**, 287-307.

Ul-Ain, Q., Sharma, S. and Khuller, G. K. (2003). Chemotherapeutic potential of orally administered poly(lactide-co-glycolide) microparticles containing isoniazid, rifampin, and pyrazinamide against experimental tuberculosis. *Antimicrob. Agents Chemother.* **47**, 3005-3007.

Yoshida, A., Matumoto, M., Hshizume, H., Oba, Y., Tomishige, T., Inagawa, H., Kohchi, C., Hino, M., Ito, F., Tomoda, K. et al. (2006). Selective delivery of rifampicin incorporated into poly(DL-lactic-co-glycolic) acid microspheres after phagocytotic uptake by alveolar macrophages, and the killing effect against intracellular Mycobacterium bovis Calmette-Guérin. *Microbes Infect.* **8**, 2484-2491.

Young, D. B., Perkins, M. D., Duncan, K. and Barry, C. E., 3rd (2008). Confronting the scientific obstacles to global control of tuberculosis. *J. Clin. Invest.* **118**, 1255-1265.

Zhang, Y. and Yew, W. W. (2009). Mechanisms of drug resistance in Mycobacterium tuberculosis. *Int. J. Tuberc. Lung Dis.* **13**, 1320-1330.